

De Novo Truncating Mutations in the Last and Penultimate Exons of *PPM1D* Cause an Intellectual Disability Syndrome

Sandra Jansen,¹ Sinje Geuer,¹ Rolph Pfundt,¹ Rachel Brough,² Priyanka Ghongane,² Johanna C. Herkert,³ Elysa J. Marco,⁴ Marjolein H. Willemsen,¹ Tjitske Kleefstra,¹ Mark Hannibal,⁵ Joseph T. Shieh,⁶ Sally Ann Lynch,^{7,8} Frances Flinter,⁹ David R. FitzPatrick,¹⁰ Alice Gardham,¹¹ Birgitta Bernhard,¹¹ Nicola Rague,^{12,13} Ruth Newbury-Ecob,¹⁴ Raphael Bernier,¹⁵ Malin Kvarnung,¹⁶ E.A. Helena Magnusson,¹⁷ Marja W. Wessels,¹⁸ Marjon A. van Slegtenhorst,¹⁸ Kristin G. Monaghan,¹⁹ Petra de Vries,¹ Joris A. Veltman,^{1,20} Deciphering Developmental Disorders Study, Christopher J. Lord,² Lisenka E.L.M. Vissers,¹ and Bert B.A. de Vries^{1,*}

Intellectual disability (ID) is a highly heterogeneous disorder involving at least 600 genes, yet a genetic diagnosis remains elusive in ~35%–40% of individuals with moderate to severe ID. Recent meta-analyses statistically analyzing de novo mutations in >7,000 individuals with neurodevelopmental disorders highlighted mutations in *PPM1D* as a possible cause of ID. *PPM1D* is a type 2C phosphatase that functions as a negative regulator of cellular stress-response pathways by mediating a feedback loop of p38-p53 signaling, thereby contributing to growth inhibition and suppression of stress-induced apoptosis. We identified 14 individuals with mild to severe ID and/or developmental delay and de novo truncating *PPM1D* mutations. Additionally, deep phenotyping revealed overlapping behavioral problems (ASD, ADHD, and anxiety disorders), hypotonia, broad-based gait, facial dysmorphisms, and periods of fever and vomiting. *PPM1D* is expressed during fetal brain development and in the adult brain. All mutations were located in the last or penultimate exon, suggesting escape from nonsense-mediated mRNA decay. Both *PPM1D* expression analysis and cDNA sequencing in EBV LCLs of individuals support the presence of a stable truncated transcript, consistent with this hypothesis. Exposure of cells derived from individuals with *PPM1D* truncating mutations to ionizing radiation resulted in normal p53 activation, suggesting that p53 signaling is unaffected. However, a cell-growth disadvantage was observed, suggesting a possible effect on the stress-response pathway. Thus, we show that de novo truncating *PPM1D* mutations in the last and penultimate exons cause syndromic ID, which provides additional insight into the role of cell-cycle checkpoint genes in neurodevelopmental disorders.

Next-generation sequencing (NGS) techniques have accelerated the discovery of genes associated with intellectual disability (ID).^{1–7} Mutations in more than 600 autosomal and X-linked genes have been implicated,⁸ but many more are likely to be elucidated. Recently, two separate meta-analyses used the de novo mutations identified in >7,000 individuals affected by a neurodevelopmental disorder to identify mutations that might also cause ID.^{9,10} In both meta-analyses, *PPM1D* (protein phosphatase, Mg²⁺/Mn²⁺-dependent 1D [MIM: 605100]),

encoding a negative regulator of cellular stress-response pathways, had significantly more damaging de novo mutations than expected given the cohort size. However, the clinical characteristics of these individuals were not provided in detail, and insights on the pathophysiological mechanism remained unidentified. Including seven individuals identified in the meta-analyses, we collected a total of 14 unrelated individuals with mild to severe ID and/or developmental delay (DD) through international collaboration with colleagues and data-sharing resources such as

¹Department of Human Genetics, Donders Centre for Neuroscience, Radboud University Medical Center, PO Box 9101, 6500 HB Nijmegen, the Netherlands; ²Cancer Research UK Gene Function Laboratory and Breast Cancer Now Research Centre, Institute of Cancer Research, London SW3 6JB, UK; ³Department of Genetics, University Medical Center Groningen, University of Groningen, PO Box 30.001, 9700 RB Groningen, the Netherlands; ⁴Departments of Neurology, Pediatrics, and Psychiatry, University of California, San Francisco, 675 Nelson Rising Lane, Suite 405, San Francisco, CA 94143, USA; ⁵Division of Pediatric Genetics, Metabolism & Genomic Medicine, University of Michigan Medical School, D5257 Medical Professional Building, 1500 East Medical Center Drive, Ann Arbor, MI 48109-5718, USA; ⁶Division of Medical Genetics, Department of Pediatrics, UCSF Benioff Children's Hospital, Institute for Human Genetics, University of California, San Francisco, San Francisco, CA 94143-0793, USA; ⁷Clinical Genetics, Children's University Hospital, Temple Street, Dublin 1, Ireland; ⁸Academic Centre on Rare Diseases, School of Medicine and Medical Sciences, University College Dublin, Dublin 1, Ireland; ⁹Department of Clinical Genetics, Guy's and St. Thomas' NHS Foundation Trust, Great Maze Pond, London SE1 9RT, UK; ¹⁰Medical Research Council Human Genetics Unit, Institute of Genetics and Molecular Medicine, University of Edinburgh, Western General Hospital, Crewe Road South, Edinburgh EH4 2XU, UK; ¹¹North West Thames Regional Genetic Service (Kennedy Galton Centre), North West London Hospitals, Watford Road, London HA1 3UJ, UK; ¹²Faculty of Health and Life Sciences, Oxford Brookes University, Gypsy Lane, Oxford OX3 0BP, UK; ¹³West Midlands Regional Clinical Genetics Service and Birmingham Health Partners, Birmingham Women's Hospital NHS Foundation Trust, Birmingham B15 2TG, UK; ¹⁴Department of Clinical Genetics, University Hospitals Bristol NHS Foundation Trust, St. Michael's Hospital, Southwell Street, Bristol BS2 8EG, UK; ¹⁵Center on Human Development and Disability, University of Washington, PO Box 357920, Seattle, WA 98195-7920, USA; ¹⁶Department of Clinical Genetics, Karolinska University Hospital Solna, Karolinska Institutet, 171 77 Stockholm, Sweden; ¹⁷Department of Medicine and Neurology, Habilitation Organization, Region Skåne, 291 89 Kristianstad, Sweden; ¹⁸Department of Clinical Genetics, Erasmus Medical Center, PO Box 2040, 3000 CA Rotterdam, the Netherlands; ¹⁹GeneDx, Gaithersburg, MD 20877, USA; ²⁰Department of Clinical Genetics, Maastricht University Medical Centre, Universiteitssingel 50, 9229 ER Maastricht, the Netherlands

*Correspondence: bert.devries@radboudumc.nl
<http://dx.doi.org/10.1016/j.ajhg.2017.02.005>

© 2017 American Society of Human Genetics.

GeneMatcher.^{9–12} One individual was previously described as part of the Simons Simplex Collection cohort.¹³ Herein, we report on an ID syndrome caused by de novo germline mutations in the last and penultimate exons of *PPM1D*, as well as the implication of such mutations in the role of *PPM1D* in stress responses.

We collected clinical data by inviting individuals back to the clinic for re-evaluation and deep phenotyping. Detailed clinical information of the 14 individuals (2–21 years old) is described in the [Supplemental Note](#) and summarized in [Table 1](#). All but one individual had mild to severe ID (93%), and 11 individuals (79%) had behavioral problems, such as anxiety disorders, attention deficit hyperactivity disorder (ADHD), obsessive behavior, sensory integration problems, and autism spectrum disorder (ASD). The individual with a normal IQ of 96 did, however, need extra tutoring at school and showed an anxiety disorder and attention problems. Seven individuals were hypersensitive for sounds. Hypotonia was a common feature in the individuals for whom this information was available (10/14 [71%]), and several individuals had a broad-based gait (5/10 [50%]). Brain MRI was performed for nine individuals (64%) without any substantial findings, except for moderate cortical and cerebellar atrophy and abnormal vascular structures in individual 13, who was also diagnosed with Potocki-Shaffer syndrome. Eight individuals (62%) had short stature, but weight and head circumference were variable. Feeding difficulties were a common feature (10/14 [71%]), and remarkably, eight individuals (62%) had periods of illness with fever and/or vomiting. In addition, nine individuals had a high pain threshold (90%). One individual had problems emerging from anesthesia. Vision problems, such as myopia, hypermetropia, and strabismus, were seen in nine individuals (64%). There was no apparent shared or consistent facial gestalt despite the presence of overlapping facial features, including a broad forehead, low-set posteriorly rotated ears, upturned nose, and broad mouth with thin upper lip ([Figure 1A](#)). Ten individuals (91%) had small hands often with brachydactyly, seven individuals had small feet, and six individuals had hypoplastic toenails. To further delineate the clinical spectrum associated with de novo mutations in *PPM1D*, we established a website to collect detailed clinical information of additional individuals to be identified over the coming year (see [Web Resources](#)).

Whole-exome sequencing was performed in all individuals as previously described,^{9,10} and all were identified to have a deleterious *PPM1D* mutation. This study was approved by the institutional review board Commissie Mensgebonden Onderzoek Regio Arnhem-Nijmegen NL36191.091.11 and received UK research ethics committee (REC) approval (10/H0305/83 granted by the Cambridge South REC and GEN/284/12 granted by the Republic of Ireland REC). Written informed consent was obtained from all individuals. Subsequent confirmation by Sanger sequencing and investigation of parental DNA

samples of 13 individuals indicated that *PPM1D* mutations had occurred de novo. Interestingly, all 14 ID-associated *PPM1D* mutations are located in the last and penultimate exons ([Figure 1B](#)) and are predicted to result in a premature stop codon in exon 6 or in the last 55 nucleotides of exon 5 ([Figure 1C](#)). The truncated mRNA is therefore presumed to escape nonsense-mediated decay (NMD) and result in a truncated PPM1D still containing its functional protein phosphatase Mg²⁺/Mn²⁺-dependent (PPM)-type phosphatase domain but lacking its nuclear localization signal (NLS). To analyze *PPM1D* mRNA expression on cDNA derived from lymphoblastoid cell lines (LCLs) of individuals with a mutation in *PPM1D*, we obtained LCLs from human blood by immortalization via Epstein-Barr virus (EBV) transformation according to standard procedures. *PPM1D* mRNA expression analysis using two different sets of primer pairs showed no significant difference in mRNA levels between control lines and cDNA derived from LCLs of individuals 2 and 3, indeed confirming that the truncated mRNA was not subjected to NMD ([Figure 2B](#)). Subsequent Sanger sequencing, performed in four individuals (1–3 and 7) with a primer set targeting the mutated area (PPM1D_1 and PPM1D_3), confirmed the presence of truncated *PPM1D* transcripts. We showed that the de novo mutations in *PPM1D* lead to stable transcription of truncated mRNA with normal expression levels. Because the truncated protein lacks its NLS, it might no longer reach the nucleus to exert its function. Immunohistochemical staining of PPM1D showed cytosolic and nuclear staining in LCLs in a control line ([Figure S1](#)). Similar staining in EBV-transformed LCLs from an individual with a heterozygous de novo mutation in *PPM1D* showed a similar localization ([Figure S1](#)). However, the latter can be explained by the presence of the wild-type allele, which still results in a fully functional PPM1D. Notably, given the specific need of PPM1D in cellular stress, it is possible that localization of the mutant PPM1D is mostly affected during this state. Further quantification of PPM1D in the different cell compartments and under different physiological scenarios could help to improve our understanding of the biological mechanism underlying *PPM1D* pathology.

Importantly, de novo mutations in *PPM1D* have not been observed in over 2,000 control trios.^{1,15–18} Interrogation of large databases, such as the Exome Aggregation Consortium (ExAC) Browser, shows that *PPM1D* is under constraint for missense mutations (*Z* score 3.13). Interestingly, however, *PPM1D* seems to be tolerant of loss-of-function mutations (with pLI = 0.00).¹⁹ Together, these scores could indicate that the pathophysiological mechanism underlying ID-associated *PPM1D* mutations is more complex and that a mechanism involving a C-terminally truncated protein is more disruptive than complete loss of it, similar to what has been identified for *DVL1* and *DVL3* frameshift mutations causing Robinow syndrome.^{20–22} This highlights the importance of not disregarding these genes without consideration, given that

Table 1. Main Clinical Features of Affected Individuals

	Individual														Total	
	1	2	3	4	5	6	7	8	9	10	11	12	13	14		
General Information																
Age	14 y	5 y	5 y	2 y	5 y	10 y	9 y, 9 m	21 y	16 y	6 y	18 y	15 y	7 y	7 y	2–21 y	
Gender	F	M	F	M	M	M	M	M	F	F	M	F	F	F	7 M, 6 F	
Mutation	c.1221T>A (p.Cys407*)	c.1216del (p.Thr406 Profs*3)	c.1260+ 1dup (p.Ser421 Thrfs*12)	c.1210C>T (p.Gln404*)	c.1269_ 1270dup (p.Glu424 Glyfs*8)	c.1339G>T (p.Glu447*)	c.1188_ 1191del (p.Asp397 Alafs*11)	c.1250dup (p.Pro418 Thrfs*16)	c.1270dup (p.Glu424 Glyfs*10)	c.1270dup (p.Glu424 Glyfs*10)	c.1281G>A (p.Trp427*)	c.1281G>A (p.Trp427*)	c.1654C>T (p.Arg552*)	c.1404_ 1411del (p.Lys469 Argfs*4)	NA	
Inheritance	de novo	de novo	de novo	de novo	de novo	de novo	de novo	de novo	de novo	de novo	de novo	de novo	NK ^a	de novo	NA	
Growth																
Birthweight (g)	2,780	4,000	2,655	3,742	3,527	3,180	2,200	2,211	3,061	2,730	3,200	3,429	NK	3,140	NA	
Height (SD)	−2.7	−1.5	−2.8	0	NK	−3	<−3	<−2.5	−2.3	−2.5	−2.7	+0.41	−2.6	−2	NA	
Weight (SD)	+2.3	+0.5	−1.9	0	NK	+2	+0.5	<−2.5	−2.2	−2	−1.8	>+2.5	−4.9	0	NA	
Head circumference (SD)	+0.7	−0.5	−1.5	−0.5	−0.5	−1	−1.8	<−2.5	−3.1	−2.5	−2.5	+3.49	NK	−1.5	NA	
Neurological																
ID (severity)	+ (mild to moderate)	+ (mild to moderate)	+ (mild)	+	+	− ^b	+ (mild to moderate)	+ (mild to moderate)	+ (severe)	+ (moderate)	+ (moderate)	+ (severe)	+ (severe)	+ (mild)	13/14 (93%)	
Hypotonia	+	+	+	+	+	−	−	+	+	+	+	−	+	−	10/14 (71%)	
Broad-based gait	+	NK	+	+	+	−	−	−	+	NK	NK	−	NK	−	5/10 (50%)	
Sensitivity to sounds	NK	NK	+	+	NK	NK	+	+	+	+	NK	NK	NK	+	7/7 (100%)	
Behavioral features	ADHD, ODD, anxiety disorder	sensory integration problems	short attention, panic attacks	sensory integration problems, hyperarousal, short attention	−	anxiety disorder, attention difficulties, biting	sensory integration problems, anxiety, short attention	anxiety	ASD	−	−	ASD, attention problems, oppositional, aggression	ASD	ASD	11/14 (79%)	
Facial																
Broad forehead	+	+	−	−	NK	−	−	+	+	+	+	NK	+	+	8/12 (67%)	
Low-set, posteriorly rotated ears	+	+	+	+	(right)	NK	NK	−	−	+	+	NK	NK	+	(only posteriorly rotated)	8/10 (80%)
Upturned nose	+	−	+	−	NK	−	−	−	−	+	+	NK	+	−	5/12 (42%)	
Thin upper lip	−	+	+	+	NK	+	−	+	+	+	+	NK	+	+	10/12 83%	
Broad mouth	+	+	+	−	NK	+	−	−	+	−	+	NK	−	−	6/12 50%	

(Continued on next page)

Table 1. Continued

	Individual														Total		
	1	2	3	4	5	6	7	8	9	10	11	12	13	14			
Gastrointestinal																	
Feeding difficulty	+ (neonatal)	+ (neonatal)	+ (neonatal)	+	+	–	+	+	–	–	+	–	+	+ (neonatal)	10/14 (71%)		
GER and/or vomiting	+	+	+	+	NK	+	+	+ (infancy)	+	+	–	–	+	–	10/13 (77%)		
Constipation	–	+	–	+	+	–	+	+ (infancy)	+	–	NK	–	+	+	8/13 (55%)		
Skeletal																	
Small hands	NK	+	+	–	NK	+	+	+	+	+	+	NK	+	+	10/11 (91%)		
Small feet	NK	NK	+	–	NK	NK	+	+	+	NK	+	NK	+	+	7/8 (88%)		
Hyperlordosis	+	–	–	–	+	NK	+	+	+	NK	+	NK	NK	+	7/10 (70%)		
Other																	
Periodic illness ^c	+	+	–	–	+	+	+	+	+	+	–	–	NK	–	8/13 (62%)		
High pain threshold	NK	+	+	+	NK	+	+	+	+	+	+	NK	NK	–	9/10 (90%)		
Congenital abnormalities	bicuspid aortic valve	retractile testes, small genital	small VSD and small ODA	–	–	bilateral cryptorchidism	–	–	–	–	laryngomalacia	–	–	bilateral parietal foramina, exostoses, diaphragmatic hernia, volvulus intestine ^d	–	6/14 (43%)	
Vision problems	myopia, nystagmus, amblyopia	hypermetropia, cilinder, strabismus	hypermetropia	myopia, strabismus, astigmatism, CVI	–	–	–	hypermetropia, strabismus, astigmatism, nystagmus	myopia, strabismus	–	–	hypermetropia, strabismus	hypermetropia, strabismus	–	strabismus, nystagmus, iridocyclitis, retinal detachment	–	9/14 (64%)
Hypoplastic nails	+ (toenails)	+ (toenails)	+ (toenails)	–	–	+ (toenails)	–	–	–	+ (fifth toenails)	–	–	+	NK	NK	–	6/12 (50%)
Recurrent infections	–	–	NK	–	NK	NK	+	NK	+	NK	+	+	+	+	–	5/9 (56%)	

Abbreviations are as follows: +, present; –, absent; y, years; m, months; M, male; F, female; NK, not known; ID, intellectual disability; ADHD, attention deficit hyperactivity disorder; ODD, oppositional defiant disorder; ASD, autism spectrum disorder; GER, gastro esophageal reflux; VSD, ventricle septum defect; ODA, open ductus arteriosus; and CVI, cerebral visual impairment.

^aParental DNA not available.

^bIndividual did have learning difficulties.

^cIncluding cyclic vomiting.

^dIndividual 13 also had a confirmed diagnosis of Potocki-Shaffer syndrome.

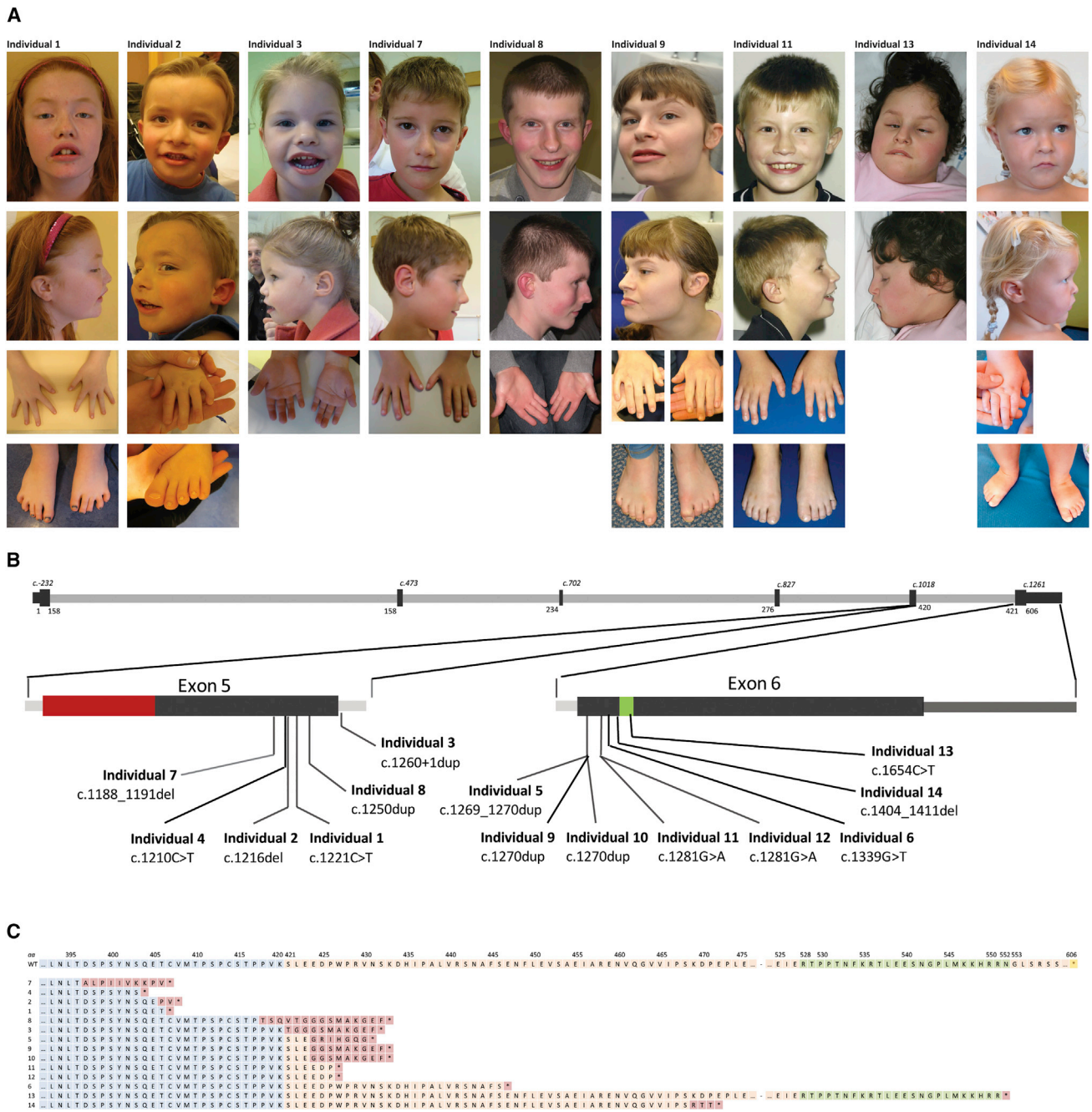


Figure 1. Photographs of Nine Individuals with a Truncating Mutation in *PPM1D*, De Novo Mutations in *PPM1D*, and Predicted Consequences at the Protein Level

(A) Shared facial features including a broad forehead, upturned nose, broad mouth with thin upper lip, and low-set posteriorly rotated ears. Extremities show small hands and feet with brachydactyly and hypoplastic toenails. Individual 13 also had a confirmed diagnosis of Potocki-Shaffer syndrome. Parents provided informed consent for the publication of these photographs.

(B) Schematic representation of the coding sequence of *PPM1D* (GenBank: NM_003620.3), including zoomed-in exons 5 and 6. All de novo *PPM1D* mutations identified are depicted according to their location in the coding sequence. Protein domain structures encoded by exons 5 and 6 are highlighted in color: red for the PPM-type phosphatase domain (in exon 5) and green for the nuclear localization signal (in exon 6).

(C) Predicted protein sequences in individuals 1–14. The last part of the translated sequence of exon 5 is in blue, and the amino acids encoded by the first part of exon 6 are in orange. For individuals 1–14, the predicted mutant amino acids are depicted in red. Abbreviations are as follows: WT, wild-type; and aa, amino acid.

the disease-causing mutations could have other pathophysiological mechanisms not directly inferable from such metrics in the ExAC Browser.

PPM1D has previously been shown to be expressed in both mouse and human brain,^{23,24} but a second hint toward a role for *PPM1D* in the occurrence of ID would

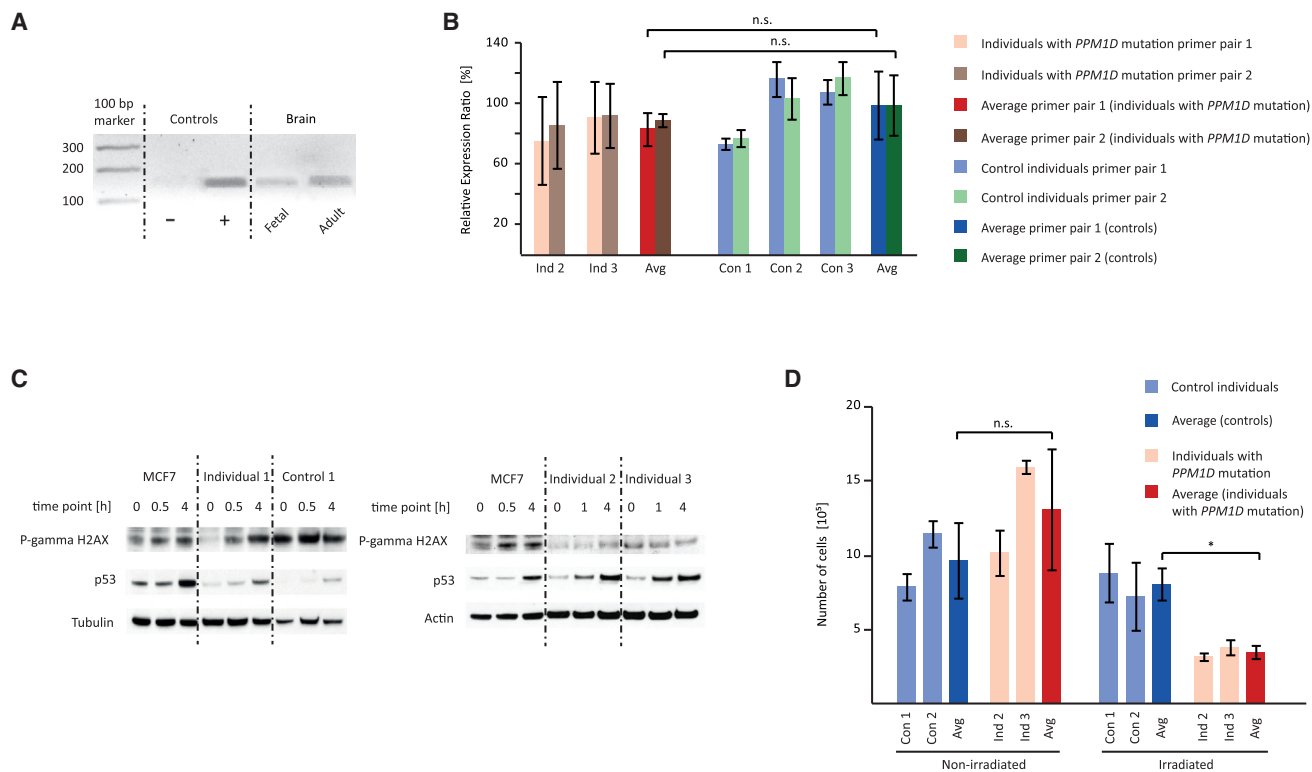


Figure 2. Functional Effects of *PPM1D* Mutations at the RNA and Protein Levels and Downstream Effects on p53 Activation and Cell Growth

(A) Semiquantitative PCR using primers *PPM1D_3* (forward: 5'-AACCTGACTGACAGCCCTTC-3'; reverse: 5'-ACCAGGGCAGGTA TATGGTC-3') on tissue-specific cDNA libraries shows *PPM1D* expression in fetal and adult brain. EBV-LCL cDNA is the positive control (+), and ddH₂O is the negative control (-).

(B) Expression levels of *PPM1D* were quantified by qPCR using cDNA obtained from EBV-LCLs derived from individuals with a mutation in *PPM1D* (individuals 2 and 3). Experiments were performed in triplicate with two sets of primer pairs: *PPM1D_1* (forward: 5'-TGC TTGTGAATCGAGCATTG-3'; reverse: 5'-CCCTGATGTCCACTTCTGG-3') and *PPM1D_2* (forward: 5'-AAGTCGAAGTAGTGGTGT CAG-3'; reverse: 5'-TCTTCTGGCCCTAAGTCTG-3'). Analysis was performed with SDS software according to standard procedures, and *GUSB* expression was used as a calibrator (forward: 5'-AGAGTGGTGCTGAGGATTGG-3'; reverse: 5'-CCCTCATGCTCTAGC GTGTC-3').¹⁴ There was no significant change in *PPM1D* mRNA expression between affected individuals and control lines. Abbreviations are as follows: n.s., not significant; Ind, individual; Con, control individual; and Avg, average. Results are presented as the average \pm SD.

(C) Radiation-induced activation of p53 was investigated in fibroblasts derived from individual 1, EBV-LCLs derived from individuals 2 and 3, healthy control cells, and the cancer cell line with active *PPM1D* (MCF7 as the positive control). Cells were exposed to gamma irradiation (5 Gy) from an X-ray source. Whole-cell lysates were generated from cells 30–60 min and 4 hr after irradiation and subjected to protein electrophoresis. Immunoblotting of electrophoresed lysates was performed with antibodies specific to p53 (9282S), phospho-Histone γ H2AX (ser139) (9718S), and actin (I-19), or β -tubulin (D-10). Anti-rabbit, anti-mouse, and anti-rabbit secondary antibodies were incubated with the blot (1:5,000) for 1 hr at room temperature, and then exposure using enhanced chemiluminescent detection followed. Western blot analysis showed no difference between case and control cell lines but did show increased p53 activation in the *PPM1D* mutant breast cancer cell line MCF7.

(D) Growth behavior of EBV-LCLs derived from individuals with a mutation in *PPM1D* (individuals 2 and 3) was compared with that of age- and sex-matched control EBV-LCLs. Cells were irradiated (UV light: 60 J/m²) and cultured in a concentration of 3×10^5 cells/mL. Cell numbers were counted in triplicate after 48 hr, and the experiment was repeated three times. 48 hr after irradiation, the number of EBV-LCLs derived from individuals with a mutation in *PPM1D* ($n = 2$) was significantly lower than that of control cells ($n = 2$), whereas the growth of untreated cells was unaffected. Abbreviations are as follows: *, $p < 0.05$; n.s., no significance; Ind, individual; Con, control individual; and Avg, average. Results are presented as the average \pm SD.

be its expression in the developing brain. We therefore investigated *PPM1D* expression in cDNA libraries obtained from fetal and adult brain by using semiquantitative PCR. Human cDNA libraries from different human tissues were purchased from Stratagene. Expression of *PPM1D* in embryonic and adult brain and EBV-LCLs (positive control) was investigated with *PPM1D*-transcript-specific semiquantitative PCR using the primer set *PPM1D_3*. We de-

tected *PPM1D* expression in both fetal and adult brain (Figure 2A). In addition, our analysis showed wider fetal (developmental), whereby *PPM1D* expression was detected in fetal liver and skeletal muscle, but not in their adult counterparts (data not shown). The expression of *PPM1D* in the fetal brain suggests a role during fetal brain development and thus potentially in developing normal cognition. Although we were not able to further narrow down

the expression to detailed brain regions, the highest *Ppm1d* expression in mice has been reported in the cerebellum,²³ which is the center for coordination. Several of our affected individuals had a broad-based gait, a possible sign of cerebellar disturbance, which might therefore be associated with the mutation in *PPM1D*. However, the individuals did not display other symptoms of coordination defects, and in the individuals who had received brain MRI, no structural abnormalities of the cerebellum could be identified.

PPM1D has also been reported to be an important regulator of global heterochromatin silencing and thus critical in maintaining genome integrity.²⁵ The latter was examined in germ cells of *Ppm1d*-deficient mice, which showed enlarged heterochromatin centers with enriched immunofluorescent staining for H3K9me3 and HP1 γ , both markers for transcriptional repression.²⁵ When *PPM1D* dysfunction indeed alters gene expression, this might have an effect on fetal (brain) development. Moreover, *Ppm1d*-deficient mice show an increase in anxiety and depression-like behavior,²⁶ suggesting a potential protective function of *PPM1D* in mood stabilization.²⁶ Interestingly, four of the individuals with a *PPM1D* mutation showed anxiety.

PPM1D (also known as *Wip1*) is, like other genes encoding PPM and PP2C phosphatases, a regulator of stress response.²⁷ In particular, *PPM1D* regulates the DNA damage response (DDR) pathway by inhibiting p53 and other tumor suppressors (p38, ATM, Chk1, and Chk2) through dephosphorylation of these proteins.²⁷ Previously substantial amounts of work have gone into the role of *PPM1D* in tumorigenesis, given that acquired *PPM1D* mutations have been identified in individuals with breast, ovarian, colon, and lung cancer and are postulated to exert their effect through gain of function.^{27–31} However, these mosaic mutations in lymphocytes were shown to occur only in individuals who had undergone chemotherapy and were shown to be absent in DNA isolated from the germline prior to chemotherapy.^{27–31} The gain-of-function effect was shown by overexpression of cancer-associated *PPM1D* mutations in tumor cells, which suppressed ionizing radiation (IR)-induced molecular responses.²⁸ In normal conditions, exposure to IR causes upregulation of p53 levels and phosphorylation of the histone H2AX (γ H2AX), events that are normally prevented by *PPM1D* activity. In tumor cells with overexpression of cancer-associated *PPM1D* mutations, p53 and γ H2AX upregulation after IR exposure is impaired, suggesting that in tumor cells, truncating *PPM1D* mutations are hyperactive.²⁸ We tested the upregulation of p53 and γ H2AX in MCF7 cells, a breast cancer cell line serving as a positive control, which showed the expected upregulation of p53 and γ H2AX, suggesting that the IR exposure was successful (Figure 2C). Compared with healthy control cells, fibroblasts from individual 1 and EBV-LCLs derived from individuals 2 and 3 showed normal p53 and γ H2AX responses (Figure 2C). In conclusion, these data indicate that ID-associated *PPM1D* mutations do not cause p53 depletion, which suggests a

pathophysiological mechanism different from the acquired *PPM1D* cancer-associated mutations.

As a regulator of the DDR, *PPM1D* plays an important role in cell-cycle control by positively upregulating G1-to-S phase progression.³² We hypothesized that the ID-associated mutations in *PPM1D* would lose this positive upregulation and thereby cause cells to stall in the G1-to-S phase, leading to reduced cell proliferation. We therefore next tested whether EBV-LCLs derived from individuals 2 and 3 showed growth abnormalities in comparison with age- and sex-matched control EBV-LCLs. For this, cells were exposed to IR and analyzed for growth characteristics (Figure 2D). Indeed, cells derived from individuals showed 50% less growth than control lines, whereas the growth of untreated cells was unaffected (Figure 2D), showing that heterozygous *PPM1D* truncation leads to growth disadvantage after radiation. Hence, if the effect of the truncating mutations in our cases is a gain of function, this does not seem to affect the role of *PPM1D* on p53. However, a cell-growth disadvantage was observed after IR, suggesting that another function related to *PPM1D* cell-cycle checkpoints might be compromised.

Several genes are known to have somatic mutations that lead to cancer but germline mutations that cause an ID phenotype. Examples include genes encoding components of the RAS-MAPK pathway, *SETBP1* (SET binding protein 1 [MIM: 611060]), and *CTNNB1* (catenin beta 1 [MIM: 116806]).^{33–36} Also, some of these germline mutations give rise to a higher cancer risk, whereas others do not.^{33–36} Germline *PPM1D* mutations in individuals with cancer have to our knowledge not yet been reported. Although it is known that germline mutations in some genes, for instance *NF1* (neurofibromin 1 [MIM: 613113]), cause ID and a higher risk of (benign) tumors,³⁷ none of the individuals studied here (2–21 years old) have developed cancer. Thus, we cannot exclude nor confirm the possibility that the *PPM1D* mutations in the individuals with ID predispose to cancer.

In conclusion, de novo truncating germline mutations in the last and penultimate exons of *PPM1D* lead to an ID syndrome with behavioral problems, hypotonia, broad-based gait, periods of fever and vomiting, high pain threshold, short stature, small hands and feet, and overlapping facial dysmorphisms. Exposure of affected cells to IR resulted in normal p53 activation, suggesting that p53 signaling is not affected by the truncated protein. Nonetheless, a cell-growth disadvantage after IR was observed. The significant enrichment of de novo mutations in individuals with ID, the expression in the developing and mature brain, and this clinical ID syndrome underscore the role of *PPM1D* in neurodevelopment.

Supplemental Data

Supplemental Data include a Supplemental Note and one figure and can be found with this article online at <http://dx.doi.org/10.1016/j.ajhg.2017.02.005>.

Conflicts of Interest

K.G.M. is an employee of GeneDx, Inc.

Acknowledgments

We thank the individuals and their parents for participating in this study. We thank Caroline Wright for her help in contacting referring clinicians from the Deciphering Developmental Disorders (DDD) study, Megan Cho for her help in contacting referring clinicians from GeneDx, Jessica Radley for clinical support, and Ms. Saskia van der Velde-Visser for culturing cells. This work was financially supported by grants from the Netherlands Organisation for Health Research and Development (917-86-319 to B.B.A.d.V., 912-12-109 to B.B.A.d.V. and J.A.V., 907-00-365 to T.K., and 918-15-667 to J.A.V.) and the European Research Council (starting grant DENOVO 281964 to J.A.V.). D.R.F. is funded by a Medical Research Council University Unit grant to the University of Edinburgh. The DDD study presents independent research commissioned by the Health Innovation Challenge Fund (grant HICF-1009-003), a parallel funding partnership among the Wellcome Trust, Department of Health, and Wellcome Trust Sanger Institute (grant WT098051). The views expressed in this publication are those of the authors and not necessarily those of the Wellcome Trust or the Department of Health. The research team acknowledges the support of the National Institute for Health Research through the Comprehensive Clinical Research Network.

Received: October 10, 2016

Accepted: February 3, 2017

Published: March 23, 2017

Web Resources

Allen Brain Atlas, <http://human.brain-map.org>
Allen Mouse Brain Atlas, <http://mouse.brain-map.org>
DECIPHER, <https://decipher.sanger.ac.uk/>
ExAC Browser, <http://exac.broadinstitute.org/>
GeneMatcher, <https://genematcher.org/>
OMIM, <http://www.omim.org/>
Our PPM1D website, <http://www.ppm1dgene.com>
RefSeq, <https://www.ncbi.nlm.nih.gov/refseq/>

References

1. Rauch, A., Wieczorek, D., Graf, E., Wieland, T., Endeke, S., Schwarzmayr, T., Albrecht, B., Bartholdi, D., Beygo, J., Di Donato, N., et al. (2012). Range of genetic mutations associated with severe non-syndromic sporadic intellectual disability: an exome sequencing study. *Lancet* *380*, 1674–1682.
2. Vissers, L.E., de Ligt, J., Gilissen, C., Janssen, I., Stehouwer, M., de Vries, P., van Lier, B., Arts, P., Wieskamp, N., del Rosario, M., et al. (2010). A de novo paradigm for mental retardation. *Nat. Genet.* *42*, 1109–1112.
3. de Ligt, J., Willemsen, M.H., van Bon, B.W., Kleefstra, T., Yntema, H.G., Kroes, T., Vulto-van Silfhout, A.T., Koolen, D.A., de Vries, P., Gilissen, C., et al. (2012). Diagnostic exome sequencing in persons with severe intellectual disability. *N. Engl. J. Med.* *367*, 1921–1929.
4. Gilissen, C., Hehir-Kwa, J.Y., Thung, D.T., van de Vorst, M., van Bon, B.W., Willemsen, M.H., Kwint, M., Janssen, I.M., Hoischen, A., Schenck, A., et al. (2014). Genome sequencing identifies major causes of severe intellectual disability. *Nature* *511*, 344–347.
5. Grozeva, D., Carss, K., Spasic-Boskovic, O., Tejada, M.I., Gecz, J., Shaw, M., Corbett, M., Haan, E., Thompson, E., Friend, K., et al.; Italian X-linked Mental Retardation Project; UK10K Consortium; and GOLD Consortium (2015). Targeted Next-Generation Sequencing Analysis of 1,000 Individuals with Intellectual Disability. *Hum. Mutat.* *36*, 1197–1204.
6. Deciphering Developmental Disorders Study (2015). Large-scale discovery of novel genetic causes of developmental disorders. *Nature* *519*, 223–228.
7. Hamdan, F.F., Srour, M., Capo-Chichi, J.M., Daoud, H., Nassif, C., Patry, L., Massicotte, C., Ambalavanan, A., Spiegelman, D., Diallo, O., et al. (2014). De novo mutations in moderate or severe intellectual disability. *PLoS Genet.* *10*, e1004772.
8. Vissers, L.E., Gilissen, C., and Veltman, J.A. (2016). Genetic studies in intellectual disability and related disorders. *Nat. Rev. Genet.* *17*, 9–18.
9. Lelieveld, S.H., Reijnders, M.R., Pfundt, R., Yntema, H.G., Kamsteeg, E.J., de Vries, P., de Vries, B.B., Willemsen, M.H., Kleefstra, T., Löhner, K., et al. (2016). Meta-analysis of 2,104 trios provides support for 10 new genes for intellectual disability. *Nat. Neurosci.* *19*, 1194–1196.
10. McRae, J.F., Clayton, S., Fitzgerald, T.W., Kaplanis, J., Prigmore, E., Rajan, D., Sifrim, A., Aitken, S., Akawi, N., Alvi, M., et al. (2016). Prevalence, phenotype and architecture of developmental disorders caused by de novo mutation. *bioRxiv*. <https://doi.org/10.1101/049056>.
11. Sobreira, N., Schiettecatte, F., Boehm, C., Valle, D., and Hamosh, A. (2015). New tools for Mendelian disease gene identification: PhenoDB variant analysis module; and GeneMatcher, a web-based tool for linking investigators with an interest in the same gene. *Hum. Mutat.* *36*, 425–431.
12. Sobreira, N., Schiettecatte, F., Valle, D., and Hamosh, A. (2015). GeneMatcher: a matching tool for connecting investigators with an interest in the same gene. *Hum. Mutat.* *36*, 928–930.
13. Sanders, S.J., Murtha, M.T., Gupta, A.R., Murdoch, J.D., Raubeson, M.J., Willsey, A.J., Ercan-Sencicek, A.G., DiLullo, N.M., PARIKSHAK, N.N., Stein, J.L., et al. (2012). De novo mutations revealed by whole-exome sequencing are strongly associated with autism. *Nature* *485*, 237–241.
14. Mukhopadhyay, A., Nikopoulos, K., Maugeri, A., de Brouwer, A.P., van Nouhuys, C.E., Boon, C.J., Perveen, R., Zegers, H.A., Wittebol-Post, D., van den Biesen, P.R., et al. (2006). Erosive vitreoretinopathy and wagner disease are caused by intronic mutations in CSPG2/Versican that result in an imbalance of splice variants. *Invest. Ophthalmol. Vis. Sci.* *47*, 3565–3572.
15. Iossifov, I., O’Roak, B.J., Sanders, S.J., Ronemus, M., Krumm, N., Levy, D., Stessman, H.A., Witherspoon, K.T., Vives, L., Patterson, K.E., et al. (2014). The contribution of de novo coding mutations to autism spectrum disorder. *Nature* *515*, 216–221.
16. Genome of the Netherlands Consortium (2014). Whole-genome sequence variation, population structure and demographic history of the Dutch population. *Nat. Genet.* *46*, 818–825.
17. Gulsuner, S., Walsh, T., Watts, A.C., Lee, M.K., Thornton, A.M., Casadei, S., Rippey, C., Shahin, H., Nimgaonkar, V.L., Go, R.C., et al.; Consortium on the Genetics of Schizophrenia (COGS); and PAARTNERS Study Group (2013). Spatial and

- temporal mapping of de novo mutations in schizophrenia to a fetal prefrontal cortical network. *Cell* 154, 518–529.
18. Xu, B., Ionita-Laza, I., Roos, J.L., Boone, B., Woodrick, S., Sun, Y., Levy, S., Gogos, J.A., and Karayiorgou, M. (2012). De novo gene mutations highlight patterns of genetic and neural complexity in schizophrenia. *Nat. Genet.* 44, 1365–1369.
 19. Lek, M., Karczewski, K.J., Minikel, E.V., Samocha, K.E., Banks, E., Fennell, T., O'Donnell-Luria, A.H., Ware, J.S., Hill, A.J., Cummings, B.B., et al.; Exome Aggregation Consortium (2016). Analysis of protein-coding genetic variation in 60,706 humans. *Nature* 536, 285–291.
 20. White, J., Mazzeu, J.F., Hoischen, A., Jhangiani, S.N., Gambin, T., Alcino, M.C., Penney, S., Saraiva, J.M., Hove, H., Skovby, F., et al.; Baylor-Hopkins Center for Mendelian Genomics (2015). DVL1 frameshift mutations clustering in the penultimate exon cause autosomal-dominant Robinow syndrome. *Am. J. Hum. Genet.* 96, 612–622.
 21. White, J.J., Mazzeu, J.F., Hoischen, A., Bayram, Y., Withers, M., Gezdirici, A., Kimonis, V., Steehouwer, M., Jhangiani, S.N., Muzny, D.M., et al.; Baylor-Hopkins Center for Mendelian Genomics (2016). DVL3 Alleles Resulting in a -1 Frameshift of the Last Exon Mediate Autosomal-Dominant Robinow Syndrome. *Am. J. Hum. Genet.* 98, 553–561.
 22. Bunn, K.J., Daniel, P., Rösken, H.S., O'Neill, A.C., Cameron-Christie, S.R., Morgan, T., Brunner, H.G., Lai, A., Kunst, H.P., Markie, D.M., and Robertson, S.P. (2015). Mutations in DVL1 cause an osteosclerotic form of Robinow syndrome. *Am. J. Hum. Genet.* 96, 623–630.
 23. Lein, E.S., Hawrylycz, M.J., Ao, N., Ayres, M., Bensinger, A., Bernard, A., Boe, A.F., Boguski, M.S., Brockway, K.S., Byrnes, E.J., et al. (2007). Genome-wide atlas of gene expression in the adult mouse brain. *Nature* 445, 168–176.
 24. Hawrylycz, M.J., Lein, E.S., Guillozet-Bongaarts, A.L., Shen, E.H., Ng, L., Miller, J.A., van de Lagemaat, L.N., Smith, K.A., Ebbert, A., Riley, Z.L., et al. (2012). An anatomically comprehensive atlas of the adult human brain transcriptome. *Nature* 489, 391–399.
 25. Filippini, D., Muller, J., Emelyanov, A., and Bulavin, D.V. (2013). Wip1 controls global heterochromatin silencing via ATM/BRCA1-dependent DNA methylation. *Cancer Cell* 24, 528–541.
 26. Ruan, C.S., Zhou, F.H., He, Z.Y., Wang, S.F., Yang, C.R., Shen, Y.J., Guo, Y., Zhao, H.B., Chen, L., Liu, D., et al. (2015). Mice deficient for wild-type p53-induced phosphatase 1 display elevated anxiety- and depression-like behaviors. *Neuroscience* 293, 12–22.
 27. Lu, X., Nguyen, T.A., Moon, S.H., Darlington, Y., Sommer, M., and Donehower, L.A. (2008). The type 2C phosphatase Wip1: an oncogenic regulator of tumor suppressor and DNA damage response pathways. *Cancer Metastasis Rev.* 27, 123–135.
 28. Ruark, E., Snape, K., Humburg, P., Loveday, C., Bajrami, I., Brough, R., Rodrigues, D.N., Renwick, A., Seal, S., Ramsay, E., et al.; Breast and Ovarian Cancer Susceptibility Collaboration; and Wellcome Trust Case Control Consortium (2013). Mosaic PPM1D mutations are associated with predisposition to breast and ovarian cancer. *Nature* 493, 406–410.
 29. Pharoah, P.D., Song, H., Dicks, E., Intermaggio, M.P., Harrington, P., Baynes, C., Alsop, K., Bogdanova, N., Cicek, M.S., Cunningham, J.M., et al.; Australian Ovarian Cancer Study Group; and Ovarian Cancer Association Consortium (2016). PPM1D Mosaic Truncating Variants in Ovarian Cancer Cases May Be Treatment-Related Somatic Mutations. *J. Natl. Cancer Inst.* 108. <http://dx.doi.org/10.1093/jnci/djv347>.
 30. Swisher, E.M., Harrell, M.I., Norquist, B.M., Walsh, T., Brady, M., Lee, M., Hershberg, R., Kalli, K.R., Lankes, H., Konnick, E.Q., et al. (2016). Somatic Mosaic Mutations in PPM1D and TP53 in the Blood of Women With Ovarian Carcinoma. *JAMA Oncol.* 2, 370–372.
 31. Zajkowicz, A., Butkiewicz, D., Drosik, A., Giglok, M., Suwiński, R., and Rusin, M. (2015). Truncating mutations of PPM1D are found in blood DNA samples of lung cancer patients. *Br. J. Cancer* 112, 1114–1120.
 32. Kleiblova, P., Shaltiel, I.A., Benada, J., Ševčík, J., Pecháčková, S., Pohlreich, P., Voest, E.E., Dundr, P., Bartek, J., Kleibl, Z., et al. (2013). Gain-of-function mutations of PPM1D/Wip1 impair the p53-dependent G1 checkpoint. *J. Cell Biol.* 201, 511–521.
 33. Niemeyer, C.M. (2014). RAS diseases in children. *Haematologica* 99, 1653–1662.
 34. Hoischen, A., van Bon, B.W., Gilissen, C., Arts, P., van Lier, B., Steehouwer, M., de Vries, P., de Reuver, R., Wieskamp, N., Mortier, G., et al. (2010). De novo mutations of SETBP1 cause Schinzel-Giedion syndrome. *Nat. Genet.* 42, 483–485.
 35. Makishima, H., Yoshida, K., Nguyen, N., Przychodzen, B., Sanada, M., Okuno, Y., Ng, K.P., Gudmundsson, K.O., Vishwakarma, B.A., Jerez, A., et al. (2013). Somatic SETBP1 mutations in myeloid malignancies. *Nat. Genet.* 45, 942–946.
 36. Kuechler, A., Willemsen, M.H., Albrecht, B., Bacino, C.A., Bartholomew, D.W., van Bokhoven, H., van den Boogaard, M.J., Bramswig, N., Büttner, C., Cremer, K., et al. (2015). De novo mutations in beta-catenin (CTNNB1) appear to be a frequent cause of intellectual disability: expanding the mutational and clinical spectrum. *Hum. Genet.* 134, 97–109.
 37. Ferner, R.E., and Gutmann, D.H. (2013). Neurofibromatosis type 1 (NF1): diagnosis and management. *Handb. Clin. Neurol.* 115, 939–955.